Letter

Dynamic interference in below-threshold ionization

Attila Tóth [1], Sándor Borbély [2], and András Csehi [3,*]

[1] *ELI-ALPS, ELI-HU Non-Profit Limited, Dugonics tér 13, H-6720 Szeged, Hungary*

[2] *Faculty of Physics, Babeş-Bolyai University, Kogălniceanu 1, RO-400084 Cluj-Napoca, Romania*

[3] *Department of Theoretical Physics, Faculty of Science and Technology, University of Debrecen, P.O. Box 400, H-4002 Debrecen, Hungary*

(Received 2 October 2023; accepted 14 November 2023; published 1 December 2023)

We study the temporal interference of photoelectrons emitted during the rising and falling edges of intense femtosecond laser pulses, that can ionize atoms via near-resonant transitions. Due to the near-resonant coupling with the laser pulse, the emerging atomic dressed states repel each other, giving rise to the Rabi splitting that is primarily controlled by the laser intensity and detuning. Our numerical and analytical analysis reveals that dynamic interference is observed when the Rabi splitting of the dressed states is maximized while the ionization of the atom remains small. We demonstrate that these two conditions are fulfilled when the atom is driven off resonantly within the one-Rabi-cycle regime at perturbative laser intensities. As a result, the single peak of the photoelectron spectrum found in the weak-field limit is replaced by a pronounced multipeak pattern.

DOI: 10.1103/PhysRevA.108.L061101

Dynamic interference (DI) of photoelectrons, a simple double-slit interference at the atomic scale, is of fundamental importance in the physics of atoms and molecules interacting with short and intense light pulses [1–3]. A clear manifestation of DI in the photoelectron spectrum is the transformation of the single photopeak into a multipeak pattern upon increasing light-matter coupling. This is attributed to the interference of electron amplitudes generated with the same energy but with a certain time delay, at the rising and falling edges of the laser pulse.

Dynamic interference has been widely studied in direct one-photon ionization processes [4–7], namely when the photon energy ω is larger than the I_p ionization potential, $\omega > I_p$ (atomic units are used unless otherwise stated). Due to the high photon frequency [extreme ultraviolet (XUV)], the laser pulse supports many optical cycles, and as a consequence the dynamical (ac) Stark shifts of the atomic levels adiabatically follow the envelope function [8]. These dynamical level shifts, induced by the laser pulse, were found to play a crucial role in DI. To observe DI, the relative Stark shift of the initial bound and final continuum states has to be maximal while the depletion of the initial state is small [2]. For ground-state atoms, dynamic interference occurs in the strongly nonperturbative region, and turns out to be closely intertwined with the onset of atomic stabilization [3].

Similar interference patterns have been observed [9,10] and predicted [11–13] in the low-frequency regime, namely when the photon energy is smaller than the ionization potential ($\omega < I_p$). In below-threshold ionization the laser can couple resonantly two bound states of the atom leading to Rabi oscillations [14]. These oscillations are best understood by way of the example of a two-level atom (with ω_0 transition energy and μ transition dipole moment) interacting with a monochromatic electric field of ω angular frequency and $\mathscr{E}_0$ amplitude [15]. The atom being initially in the ground state is periodically excited to the upper level with probability $P(t) = \frac{\Omega^2}{W^2}\sin^2(Wt/2)$. Here, $W = \sqrt{\Omega^2 + \Delta^2}$ is the generalized Rabi frequency with $\Delta = \omega - \omega_0$ detuning and $\Omega = \mathscr{E}_0\mu$ Rabi frequency. Due to the near-resonant coupling with the laser, two atomic dressed states are formed, the energy separation (Rabi splitting) of which equals W. In the case of laser pulses, the Rabi dynamics is somewhat altered (e.g., Gaussian pulses induce ∼1.5 times more oscillations than flattop pulses with the same area), and furthermore, the splitting of the dressed-state energies becomes time dependent according to the envelope function. Upon absorption of further photon(s) from the same pulse, the Rabi oscillations are damped due to ionization, and the Autler-Townes (AT) doublet is formed in the spectrum [16]. The structure of the AT doublet is very sensitive to different physical circumstances such as the number of Rabi cycles completed by the system [17–22], the ac Stark shifts of the involved atomic levels [23,24], the energy dependence of the bound-continuum transition dipoles [25], the shape of the pulse envelope [22,24], the phase of the driving field [26–28], or the interplay between the resonant and nonresonant ionization pathways [15,29].

There has been a debate over whether the multipeak pattern found in the AT doublet after resonance ionization results from the interference of electron amplitudes generated at the rising and falling edges of the laser pulse [19], or if it is the manifestation of Rabi oscillations between the resonantly coupled states [22]. The analysis carried out in the stationary phase approximation (SPA) suggested that the spectra calculated with half pulses do not possess any intensity modulation, and led to the conclusion that the multipeak pattern obtained with the full pulse is the result of dynamic interference [19]. The absence of such intensity modulations is most probably due to omitting one of the dressed states in the analytical spectrum formula. When both dressed states are included,

*csehi.andras@science.unideb.hu

the intensity modulations are retained in the spectra calculated with half pulses in the SPA [30]. This is supported by accurate numerical calculations [22]: When applying a half Gaussian pulse, or a flattop pulse (that has no rising nor falling edge), pronounced intensity modulations are still present in the spectra. Therefore, the multipeak pattern of the AT doublet obtained with the full pulse cannot be attributed exclusively to dynamic interference.

Motivated by the aim to demonstrate a clear fingerprint of dynamic interference in resonance ionization, we focus here on the one-Rabi-cycle regime, namely when the atom completes no more than one Rabi flopping during the interaction with the laser pulse [Figs. 1(a) and 1(b)]. In this regime, a single peak is expected in the photoelectron spectrum, and the impact of further Rabi floppings is safely ruled out. To be specific, we consider the $1s \to 2p \to$ continuum ionization pathway of the hydrogen atom, which has been the subject of numerous studies over the past years [19,20,22,25,29,31,32]. Linearly polarized Gaussian laser pulses along the z direction are applied in the numerical calculations,

$$\mathscr{E}(t) = \mathscr{E}_0 g(t)\cos(\omega t), \tag{1}$$

with the envelope function $g(t) = e^{-t^2/T^2}$. Here, T is the pulse duration parameter that is closely related to the full width at half maximum FWHM $= T\sqrt{2\ln 2}$.

To provide quantitative conditions for dynamic interference in below-threshold ionization, we introduce a minimal effective model that is able to accurately describe the underlying physics. The total time-dependent wave function of the electron is written in the basis of the (bound and continuum) eigenstates of the atom, classifying them into essential ($1s$, $2p$, ε) and nonessential (m),

$$\Psi(t) = c_{1s}(t)|1s\rangle e^{-i\omega_{1s}t} + c_{2p}(t)|2p\rangle e^{-i\omega_{2p}t} + \cancel{\sum} c_m(t)|m\rangle e^{-i\omega_m t} + \int c_\varepsilon(t)|\varepsilon\rangle e^{-i\omega_\varepsilon t} d\omega_\varepsilon. \tag{2}$$

Here, ε denotes all the continuum states that are populated during the dynamics, and m denotes all the states (bound and continuum) that have a net population close to zero. Inserting Eq. (2) into the time-dependent Schrödinger equation (TDSE) $i\dot{\Psi} = [H_0 + z\mathscr{E}(t)]\Psi$, one obtains the minimal effective model after some algebra and well-justified approximations [for details of the derivation, see Supplemental Material (SM) [30]],

$$i\dot{c}_{1s} = S_{1s}g^2(t)c_{1s} + \frac{1}{2}\Omega g(t)c_{2p}, \tag{3a}$$

$$i\dot{c}_{2p} = \frac{1}{2}\Omega^\dagger g(t)c_{1s} + \left[\left(S_{2p} - i\frac{\Gamma}{2}\right)g^2(t) - \Delta\right]c_{2p}, \tag{3b}$$

$$i\dot{c}_{\varepsilon s/\varepsilon d} = \frac{1}{2}\Omega_{s/d}g(t)c_{2p} - (\Delta + \delta)c_{\varepsilon s/\varepsilon d}. \tag{3c}$$

The most relevant parameters of this model, such as the Δ detuning, the Ω Rabi frequency, and the Γ ionization rate, scale with the zeroth, first, and second powers of $\mathscr{E}_0$, respectively. The S_k Stark shifts of the bound levels are expected to play a crucial role in multiphoton transitions [24], but here we kept them to improve the accuracy of the model. Finally, in Eq. (3c), Ω_l is the Rabi frequency and δ is the corresponding detuning for the transition from $|2p\rangle$ to the continuum state $|\varepsilon l\rangle$ (that has energy ω_ε and parity $l = s, d$). As will be clear below (in Fig. 3), for the laser parameter values considered here, the spectra calculated from Eqs. (3a)–(3c) as $w(\omega_{\varepsilon l}) = |c_{\varepsilon l}(t \to \infty)|^2$ are nicely supported by those obtained from the accurate numerical solution of the TDSE (details of the full calculations are given in SM [30]). This allows us to use the model for assessing the conditions for DI.

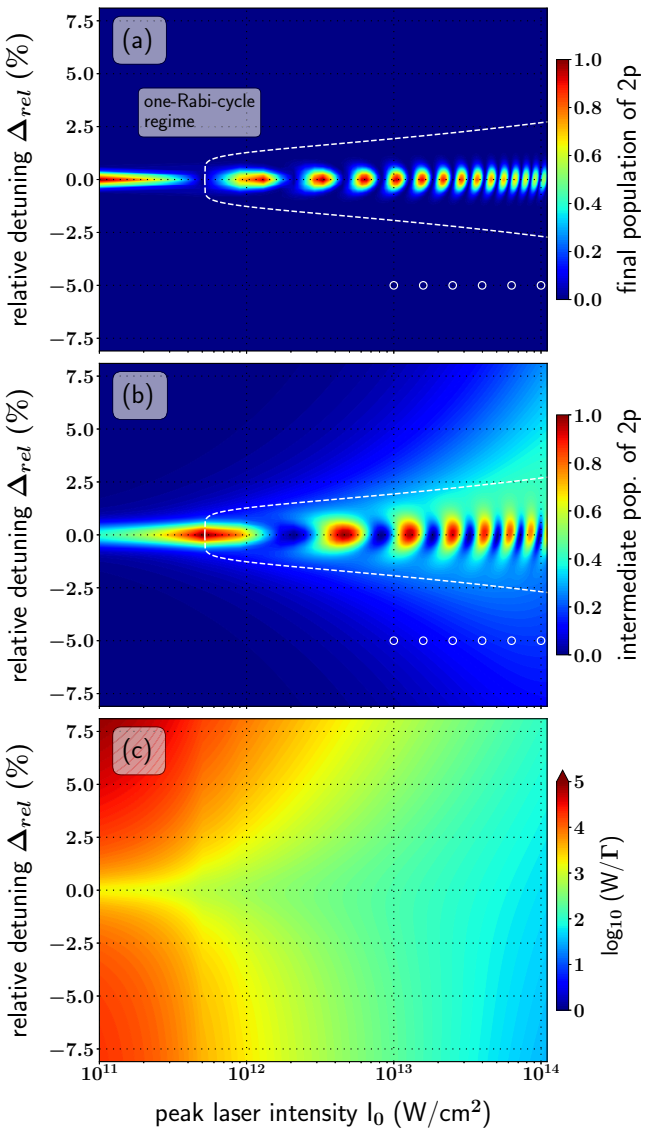

FIG. 1. Sequential two-photon ionization of hydrogen by Gaussian pulses of $T = 30$ fs duration set to near resonance with the $1s$-$2p$ transition ($\omega_{\rm res} = 3/8$ a.u. ≈ 10.204 eV). Shown are the populations of the $2p$ state (a) when the pulse has expired and (b) when the pulse is maximal. The white dashed lines indicate the boundary between the laser parameter regions where the atom completes a single or multiple Rabi cycles. (c) Ratio of the $1s$-$2p$ Rabi splitting (W) and the ionization rate of the $2p$ state (Γ). The necessary condition for dynamic interference [Eq. (6)] is well satisfied in the whole parameter range considered ($W \gg \Gamma$). The open circles indicate the laser parameters at which the spectra are calculated in Figs. 3(c) and 3(d).

Dynamic interference is expected to dominate the spectrum if (1) the energy splitting of the dressed states is large

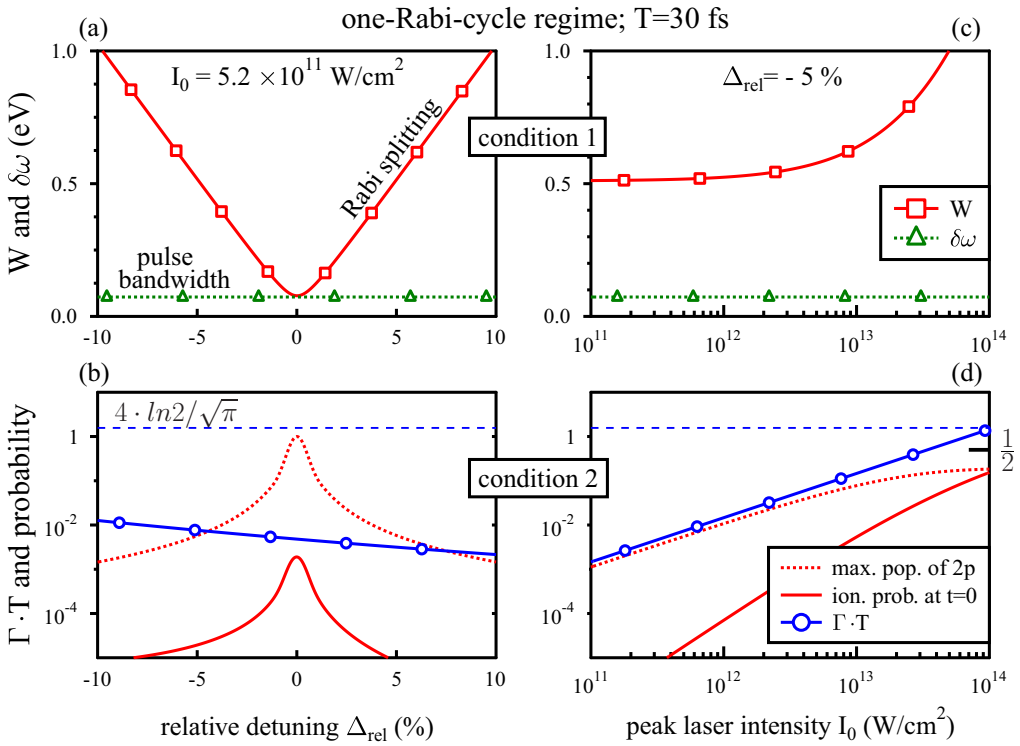

FIG. 2. Conditions for dynamic interference in the one-Rabi-cycle regime for different laser intensities and detunings. (a) Detuning dependence of condition 1 [Eq. (4)] : Resonant pulses do not and off-resonant pulses do satisfy condition 1. (b) Detuning dependence of condition 2 [Eq. (5)]: Although condition 2 is well satisfied at any detuning value, far off-resonant driving leads to marginal excitation and ionization probabilities. (c), (d) Intensity dependence of conditions 1 and 2, respectively, for a fixed detuning value ($\Delta_{rel} = -5\%$): (c) For increasing intensity, condition 1 is always satisfied; (d) condition 2 might be violated at very strong couplings. The threshold for condition 2 is underestimated by the simple analytical formula of Eq. (5) (solid blue line with circles, $\sim 1 \times 10^{14}$ W/cm^2) in contrast to the numerical prediction $P_{ion}(t = 0) < 1/2$ (solid red line, $> 1 \times 10^{14}$ W/cm^2).

enough compared to the pulse bandwidth (for a proper energetic resolution), and furthermore, if (2) the depletion of the atom remains moderate (to have ionization at both edges of the pulse). To quantify condition 1, the right-hand sides of Eqs. (3a) and (3b) are diagonalized to obtain the Rabi splitting $W = \sqrt{\Omega^2 + (\delta S - \Delta)^2}$ which is slightly modified by the $\delta S = S_{2p} - S_{1s}$ relative Stark shift [33]. Utilizing the bandwidth of the applied Gaussian pulse, $\delta\omega = 4\sqrt{\ln 2}/T$, condition 1 is written as

$$W > \frac{4\sqrt{\ln 2}}{T}. \tag{4}$$

Since no exact analytic solution is known to the problem of a two-level atom driven by a detuned Gaussian laser pulse [34], to quantify condition 2, we estimate the ionization probability with a flattop pulse that has the same area as the Gaussian counterpart, namely a duration of $T\sqrt{\pi}$. Making use of the maximal occupation of the excited level $\frac{\Omega^2}{W^2}$, and that $-\frac{\Gamma}{2}\int_{-\infty}^{\infty} g^2(t)dt = -\frac{\Gamma}{2}T\sqrt{\pi}$ for flattop pulses, the ionization probability at the center of the pulse can be estimated as $P_{ion}(\Delta, I_0) \simeq \frac{\Omega^2}{W^2}[1 - e^{-\frac{\Gamma}{4}T\sqrt{\pi}}]$. This simple analytical expression for $P_{ion}(\Delta, I_0)$ safely overestimates the exact value at any Δ and I_0. Thus $P_{ion}(\Delta, I_0)$ is expected to provide a lower bound for the depletion condition. Finally, condition 2 $[P_{ion}(\Delta, I_0) < 1/2]$ is written as

$$\Gamma T < \frac{4}{\sqrt{\pi}} \ln\left(\frac{2\Omega^2}{\Omega^2 - (\delta S - \Delta)^2}\right). \tag{5}$$

In general, for far off-resonant driving $[(\delta S - \Delta)^2 > \Omega^2]$ the excitation probability and thus the ionization yield is marginal and hence condition 2 is automatically fulfilled. On the other hand, within the domain of Eq. (5) $[(\delta S - \Delta)^2 < \Omega^2]$ the right-hand side can be simplified by taking its minimal value $(\Gamma T < 4 \ln 2/\sqrt{\pi})$. Then the necessary condition for DI is found from Eqs. (4) and (5),

$$W > \sqrt{\frac{\pi}{\ln 2}}\Gamma, \tag{6}$$

implying that the Rabi splitting should dominate over the ionization rate. As seen in Fig. 1(c), Eq. (6) is fulfilled for all values of the relative detuning ($\Delta_{rel} = \Delta/\omega_{res}$) and peak laser intensity considered ($W \gg \Gamma$). Besides Eq. (6), however, the individual criteria in Eqs. (4) and (5) has to be satisfied too. As seen in Fig. 2(a)—and also from a further evaluation of Eq. (4)—resonant pulses do not satisfy condition 1, though they satisfy condition 2. As a consequence, the spectra calculated for $\Delta = 0$ and for different laser intensities in the one-Rabi-cycle regime [keeping the pulse area constant,

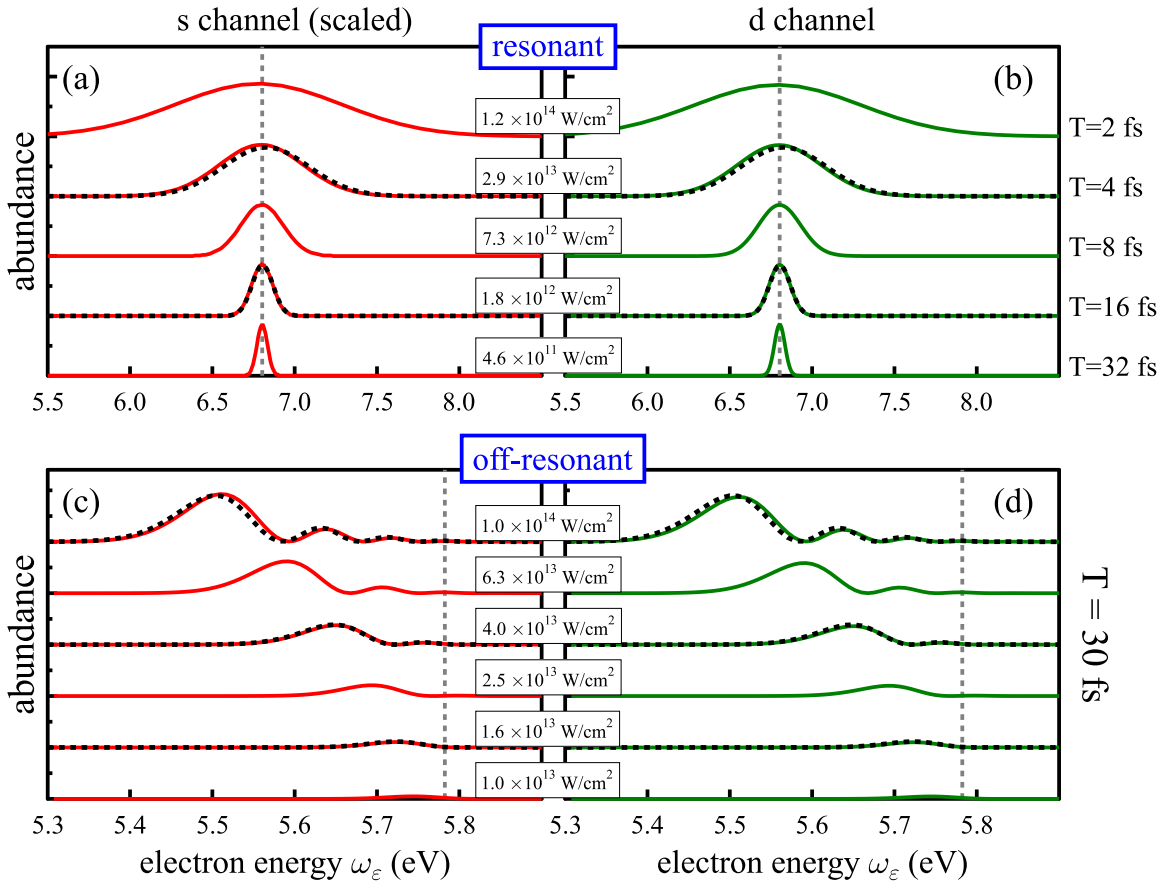

FIG. 3. Photoelectron spectra of hydrogen after sequential two-photon ionization, induced by (a), (b) resonant and (c), (d) off-resonant pulses in the one-Rabi-cycle regime. (a), (b) Resonant pulses ($\omega = 0.375$ a.u.) do not satisfy condition 1 [Eq. (4)] and thus the spectra possess no intensity modulations. Here, the laser parameters are chosen to keep the pulse area constant ($\theta = 2\pi$). (c), (d) For off-resonant pulses ($\Delta_{\rm rel} = -5\%$), the atom still completes no more than one Rabi cycle (see Fig. 1), and furthermore, conditions 1 and 2 are simultaneously fulfilled (see Fig. 2), allowing dynamic interference to come into play. This is manifested in the pronounced intensity modulations of the spectra for increasing coupling strength (both in the s and d channels). Here, the laser intensities are chosen according to $I_0(k) = 10^{k/5} \times 10^{13}$ W/cm^2 ($k = 0, 1, \ldots, 5$). For better visualization the spectra are shifted apart from each other, and the spectra in the s channel are multiplied by a factor of $|\mu_{2p\varepsilon_0 d}|^2/|\mu_{2p\varepsilon_0 s}|^2$ to have identical peak heights in the perturbative limit. The vertical dashed lines indicate the nominal positions of the spectra $\omega_{\varepsilon_0} = \omega_{1s} + 2\omega$ expected in the weak-field limit. The solid lines represent the full solution of the TDSE in the length gauge (multilevel method [30]) while the model solutions [Eqs. (3a)–(3c)] are shown by the dashed curves.

$\theta = \int_{-\infty}^{\infty} \mathcal{E}_0 \mu g(t) dt = \mathcal{E}_0 \mu \sqrt{\pi} T = 2\pi$] do not possess any intensity modulation in Figs. 3(a) and 3(b).

On the contrary, for off-resonant driving both conditions are fulfilled simultaneously [Figs. 2(a) and 2(b)], but the price one pays is that the ionization probabilities become marginal [Fig. 2(b)]. This is easily compensated by increasing the laser intensity, which further facilitates the fulfillment of condition 1 [see Fig. 2(c)]. Driving the system off resonantly ($\Delta_{\rm rel} = -5\%$) with strong pulses ($I_0 > 10^{13}$ W/cm^2) enables dynamic interference to come into play, as clearly demonstrated by the pronounced intensity modulations of the spectra in Figs. 3(c) and 3(d). For such laser parameter values the depletion condition is still satisfied [Fig. 2(d)], meanwhile the Rabi splitting well exceeds the pulse bandwidth [Fig. 2(c)]. Though the threshold for condition 2 is underestimated by the simple analytical model ($\sim 1 \times 10^{14}$ W/cm^2), the numerical simulations provide a more accurate prediction ($> 1 \times 10^{14}$ W/cm^2). The conditions for DI are thus clearly satisfied on the boundary of the linear regime, en route to the nonperturbative region, and as a result the single photopeak of the spectrum, found in the weak-field limit, turns into a multipeak pattern (both in the s and d channels).

The time evolution of the spectrum during the interaction with the laser pulse is shown in Fig. 4 for the strongest coupling considered [uppermost spectrum in Figs. 3(c) and 3(d)]. On the rising edge of the pulse ($t < 0$) the splitting of the dressed states is increasing as the pulse envelope function and accordingly electrons are emitted with different kinetic energies. For early times, the spectrum is symmetric around the nominal spectrum position $\omega_{\varepsilon_0} = 5.7824$ eV, and then gradually gets shifted towards lower energies. On the falling edge of the pulse ($t > 0$)—in the second arm of the interferometer—the energy splitting decreases and the kinetic energy gained by the emitted electrons equals that gained at the rising edge. As all the conditions are satisfied, dynamic interference becomes operational, giving rise to strong intensity modulations in the spectrum, which develop at the falling edge, and remain observable after expiration of the pulse [1].

In summary, we have provided quantitative conditions for dynamic interference in below-threshold ionization, on the

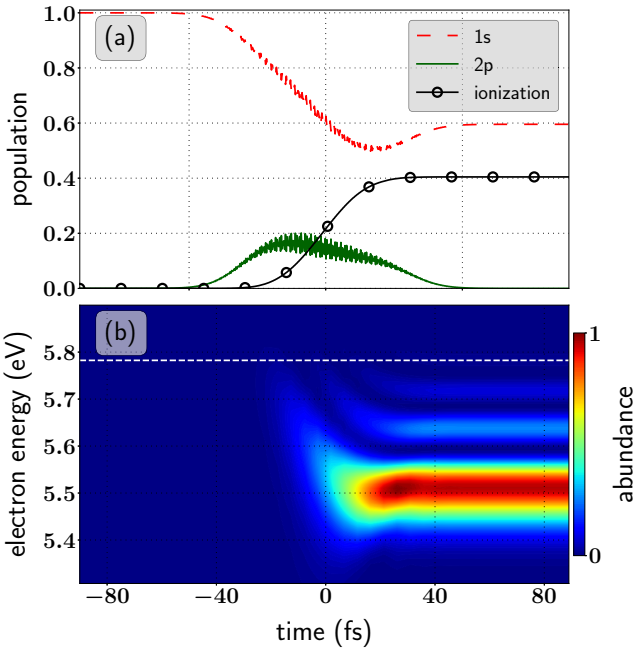

FIG. 4. (a) Time evolution of the electronic state populations and (b) of the corresponding total photoelectron spectrum of hydrogen, induced by a single Gaussian laser pulse of $T = 30$ fs duration, $\omega \approx 9.694$ eV carrier frequency ($\Delta_{\rm rel} = -5\%$), and $I_0 = 1 \times 10^{14}$ W/cm^2 peak intensity [see the uppermost spectra in Figs. 3(c) and 3(d)]. On the rising edge of the pulse but before its maximum ($t < 0$) the spectrum is nearly symmetric, and its maximum is gradually shifted away from the nominal spectrum position ($\omega_{\varepsilon_0} = \omega_{1s} + 2\omega$, white dashed line). On the falling edge of the pulse after its maximum ($t > 0$), pronounced intensity modulations start to develop in the spectrum, similarly to that reported previously for one-photon ionization [1]. The presented results are obtained by the multilevel method [30].

basis of accurate numerical simulations, a minimal level description, and analytical considerations. These conditions can be considered a natural extension of those found previously in direct one-photon ionization [2]. We have shown that dynamic interference becomes operational when the Rabi splitting of the atomic dressed states well exceeds the pulse bandwidth while the depletion of the atom is small. This is achieved when the atomic transition is driven off resonantly at sufficiently strong coupling. Focusing on the one-Rabi-cycle regime, the impact of Rabi floppings could be eliminated, allowing dynamic interference to dominate the spectrum. The pronounced intensity modulations of the spectrum were shown to develop upon a transition from the linear towards the nonperturbative regime. Interestingly, these spectral modulations are weakly modified by the ac Stark shifts of the involved bound and continuum levels [30]. It is an intriguing question how dynamic interference modifies the spectrum beyond the one-Rabi-cycle regime, where multiple Rabi oscillations are also manifested in the AT doublet. Furthermore, it is of great interest for future studies how nonperturbative phenomena, such as the competition of multiphoton ionization pathways [15], or stabilization [3] in the below-threshold regime [35,36], affect the temporal interference effect discussed in this Letter.

A.C. is grateful for the support of the János Bolyai Research Scholarship No. (BO/00474/22/11) of the Hungarian Academy of Sciences. This work was supported by the ÚNKP-23-5 New National Excellence Program of the Ministry for Culture and Innovation from the source of the National Research, Development and Innovation Fund. The ELI-ALPS Project No. (GINOP-2.3.6-15-2015-00001) is supported by the European Union and cofinanced by the European Regional Development Fund. The authors are indebted to NKFIH for funding (Grant No. K128396).

[1] P. V. Demekhin and L. S. Cederbaum, Phys. Rev. Lett. **108**, 253001 (2012).
[2] M. Baghery, U. Saalmann, and J. M. Rost, Phys. Rev. Lett. **118**, 143202 (2017).
[3] W.-C. Jiang and J. Burgdörfer, Opt. Express **26**, 19921 (2018).
[4] K. Toyota, O. I. Tolstikhin, T. Morishita, and S. Watanabe, Phys. Rev. A **76**, 043418 (2007); **78**, 033432 (2008).
[5] O. I. Tolstikhin, Phys. Rev. A **77**, 032712 (2008).
[6] A. N. Artemyev, A. D. Müller, D. Hochstuhl, L. S. Cederbaum, and P. V. Demekhin, Phys. Rev. A **93**, 043418 (2016).
[7] W.-C. Jiang, S.-G. Chen, L.-Y. Peng, and J. Burgdörfer, Phys. Rev. Lett. **124**, 043203 (2020).
[8] B. J. Sussman, Am. J. Phys. **79**, 477 (2011).
[9] R. R. Freeman, P. H. Bucksbaum, H. Milchberg, S. Darack, D. Schumacher, and M. E. Geusic, Phys. Rev. Lett. **59**, 1092 (1987).
[10] R. R. Jones, Phys. Rev. Lett. **74**, 1091 (1995).
[11] V. C. Reed and K. Burnett, Phys. Rev. A **43**, 6217 (1991).
[12] M. Wickenhauser, X. M. Tong, and C. D. Lin, Phys. Rev. A **73**, 011401(R) (2006).
[13] Y. Zhao, Y. Zhou, J. Liang, Q. Ke, Y. Liao, M. Li, and P. Lu, Phys. Rev. A **106**, 063103 (2022).
[14] I. I. Rabi, Phys. Rev. **51**, 652 (1937).
[15] S. Nandi, E. Olofsson, M. Bertolino, S. Carlström, F. Zapata, D. Busto, C. Callegari, M. Di Fraia, P. Eng-Johnsson, R. Feifel, G. Gallician, M. Gisselbrecht, S. Maclot, L. Neoričić, J. Peschel, O. Plekan, K. C. Prince, R. J. Squibb, S. Zhong, P. V. Demekhin, M. Meyer *et al.*, Nature (London) **608**, 488 (2022).
[16] S. H. Autler and C. H. Townes, Phys. Rev. **100**, 703 (1955).
[17] D. Rogus and M. Lewenstein, J. Phys. B: At. Mol. Phys. **19**, 3051 (1986).
[18] C. Meier and V. Engel, Phys. Rev. Lett. **73**, 3207 (1994).
[19] P. V. Demekhin and L. S. Cederbaum, Phys. Rev. A **86**, 063412 (2012).
[20] A. D. Müller, E. Kutscher, A. N. Artemyev, L. S. Cederbaum, and P. V. Demekhin, Chem. Phys. **509**, 145 (2018).
[21] D. A. Tumakov, D. A. Telnov, G. Plunien, and V. M. Shabaev, Phys. Rev. A **100**, 023407 (2019).
[22] N. S. Simonović, D. B. Popović, and A. Bunjac, Atoms **11**, 20 (2023).
[23] A. Tóth and A. Csehi, J. Phys. B: At., Mol. Opt. Phys. **54**, 035005 (2021).
[24] A. Tóth, S. Borbély, Y. Zhou, and A. Csehi, Phys. Rev. A **107**, 053101 (2023).

[25] A. Bunjac, D. B. Popović, and N. S. Simonović, Eur. Phys. J. D **76**, 249 (2022).
[26] M. Wollenhaupt, A. Assion, O. Bazhan, Ch. Horn, D. Liese, Ch. Sarpe-Tudoran, M. Winter, and T. Baumert, Phys. Rev. A **68**, 015401(R) (2003).
[27] T. Bayer, M. Wollenhaupt, H. Braun, and T. Baumert, Adv. Chem. Phys. **159**, 235 (2016).
[28] T. Bayer, K. Eickhoff, D. Köhnke, and M. Wollenhaupt, Phys. Rev. A **108**, 033111 (2023).
[29] X. Zhang, Y. Zhou, Y. Liao, Y. Chen, J. Liang, Q. Ke, M. Li, A. Csehi, and P. Lu, Phys. Rev. A **106**, 063114 (2022).
[30] See Supplemental Material at http://link.aps.org/supplemental/10.1103/PhysRevA.108.L061101 for (1) the derivation of the minimal effective model; (2) demonstration of the impact of bound-state ac Stark shifts on the spectra; (3) description of the numerical calculations; (4) comparison of the spectra obtained in the length and velocity gauges; and (5) evaluation of the spectrum in the stationary phase approximation.
[31] K. J. LaGattuta, Phys. Rev. A **47**, 1560 (1993).
[32] M. G. Girju, K. Hristov, O. Kidun, and D. Bauer, J. Phys. B **40**, 4165 (2007).
[33] For example, for $\Delta_{\rm rel} = -5\%$ and $I_0 = 7.2 \times 10^{13}\,{\rm W/cm^2}$, W is underestimated by 9.5% when δS is neglected.
[34] G. S. Vasilev and N. V. Vitanov, Phys. Rev. A **70**, 053407 (2004).
[35] B. L. Beers and L. Armstrong, Phys. Rev. A **12**, 2447 (1975).
[36] E. Olofsson and J. M. Dahlström, Phys. Rev. Res. **5**, 043017 (2023).